

Experimental Investigation of X-Ray Radiation Shielding and Radiological Properties for Various Natural Composites

Sonal Varshney^{1,2*}, Lalit Kumar³, Umesh K Dwivedi¹, Pradeep Narayan⁴

Abstract

Background: Shielding from radiation and plan dose verification is vital during the potential applications in industrial and medical applications. A number of natural composites have been investigated for protecting against high-energy X-ray shielding. **Objective:** The aim is to learn about how natural composites behave under various X-ray energies at STP. **Material and Methods:** The radiological parameters of wood samples were determined using computed tomography imaging, specifically relative electron density (RED), Hounsfield units (HUs), and mass density (MD). Percentage attenuation was measured using a semiflux ionization chamber incorporated with a brass build-up cap and an ionization chamber placed at the beam Isocenter for a different type of natural composite. Measurements are being carried out on a Linear accelerator at an SSD of 110 cm with different collimator sizes. **Results:** Measured values of HUs, RED, and MD were -232 ± 40 , 0.738 ± 0.039 , 0.768 ± 0.024 g/cc, -368 ± 41 , 0.662 ± 0.047 , 0.632 ± 0.024 g/cc, -334 ± 44 , 0.639 ± 0.042 , 0.666 ± 0.026 g/cc, -370 ± 61 , 0.604 ± 0.059 , 0.63 ± 0.036 g/cc, -433 ± 39 , 0.543 ± 0.038 , 0.608 ± 0.035 g/cc, -382 ± 54 , 0.5 ± 0.052 , 0.618 ± 0.0316 g/cc, -292 ± 68 , 0.680 ± 0.066 , 0.708 ± 0.039 g/cc, -298 ± 27 , 0.680 ± 0.0229 , 0.702 ± 0.131 g/cc, for Acacia Nilotica, Mangifera Indica, Azadirachta Indica, Tectona Grandis L, Ficus Religiosa, Tecomella Undulata, Sesamum Indicum, Pinus respectively. **Conclusion:** Measurements show that attenuation is affected by the energy of incident photons, collimator opening, and the type of density of the wood. Various radiological parameters were determined for wood samples that can be utilized to create inhomogeneous phantoms in dosimetry. The largest attenuation is found in Acacia Nilotica and Sesamum Indicum, while the lowest attenuation is found in Ficus religiosa.

Keywords: X-rays- woods- ionization chamber- dosimetry- radiation- LINAC

Asian Pac J Cancer Prev, 24 (10), 3555-3561

Introduction

The discovery of radiation is a boon for mankind. Radiation interactions with the matter have become increasingly widespread and fascinating in recent years (Attix, 2008). Radiation has many applications in all spheres of human life viz., industry, electricity, national security, agriculture, food, fluid fuel substitute, environment and health, etc. In the health sector, radiation is mainly used for the diagnosis of diseases and cancer radiation-therapy applications. Aside from uses, radiation has a serious detrimental effect on human health (Charles, 2008). Table 1 shows some of the radiation effects on different regions of the human body. This biological effect depends on the amount of radiation exposure, part of the body, radiation characteristics, and biological variability of tissue exposed to radiation (Charles, 2008; BOARD, 1996). Therefore, radiation protection becomes a vital need of the hour for the safe use of radiation energy. The basic principle of radiation protection is justification (risk versus benefits), optimization of radiation doses as low as

reasonably achievable (ALARA), and dose limits to be followed as stipulated by national/international regulatory bodies (Charles, 2008; Martin et al., 2018). The basic approach to achieving protection against radiation is time, distance, and shielding. Shielding is a crucial component of radiation protection and must be adequate enough. The amount of shield requires to provide safety which is dependent on the material used and incident radiation energy. Henceforth, advances in shielding material and structure technology are required to protect human beings from unwanted radiation exposure (International Atomic Energy Agency, 2006).

Innovative and new shielding materials are required to emphasize on radiation shielding efficiency and structural integrity. Desired attenuation, thickness, heat dissipation, resistance to radiation damage, cost, and weight are the desired features of shielding material. Lead, Aluminum, and concrete have been extensively used for shielding against radiation (International Atomic Energy Agency, 2006). Wood and its composite can also be used as a shielding material against radiation. A wooden door of

¹Department of Physics, Amity School of Applied Sciences, Amity University Rajasthan, Jaipur (India). ²Department of Radiation Oncology, All India Institute of Medical Sciences, Jodhpur, Rajasthan, India. ³Department of Radiation Oncology, Max Super Specialty Hospital, Saket, New Delhi, India. ⁴Defence Laboratory, DRDO Jodhpur, India. *For Correspondence: sonalvarshney18@gmail.com

various thicknesses has been used most often in X-ray diagnostic centers around the globe. Apart from this, wood has been reported to be used in the fabrication of heterogeneous phantom for dose verification in various dosimetric studies, and in testing the intrinsic behaviors of dose computation algorithms used in radiation therapy clinical settings (Kishore et al., 2020; Kumar et al., 2022). Wood has been classified as soft (from conifers) and hardwood (other than conifers). Wood and wood-derived materials have been explored in the literature. However, their potential uses are still under-rated and need to be thoroughly investigated for their physical, mechanical, and chemical processes. The aim of the present study is to investigate how natural composites of wood respond under varied X-ray energies at standard temperatures and pressures (STP). The radiological properties viz. linear attenuation coefficient, mass attenuation coefficient, relative electron density, Hounsfield units (HU), and mass density were also studied for *Acacia Nilotica*, *Mangifera Indica*, *Azadirachta Indica*, *Tectona Grandis L*, *Ficus Religiosa*, *Tecomella Undulata*, *Sesamum Indicum* and *Pinus*.

Materials and Methods

Wood Sample Collection

In this experimental study, eight different types of fresh wood available in Rajasthan, India were procured with the help of local suppliers. These samples have different types, family, scientific and common names enlisted in Table 2. These samples of wood were first dried at 30°C for approximately 60 days and then converted into experimental samples of specific sizes as mentioned in Table 3. Wood is cut transversely at the mid stem of the tree and then transformed into the necessary samples in order to prevent inhomogeneity in the sample surface and its texture. Additionally, throughout the drying process, weight and moisture stability are continuously evaluated.

Acquiring Computed Tomography (CT) images

A computed tomography (CT) scan was performed using the GE Optima 580w CT Scanner (GE Medical System, US). The acquisition was carried out in accordance with the standard head and neck scanning protocol, with the following parameters: field-of-view (FOV) 50 cm, tube voltage 120 kVp, tube current 248 mA, scan time 1.0 sec, and slice thickness 1.25 mm. All CT images were transferred to the Monaco treatment planning system (TPS) in the digital imaging and communication in medicine (DICOM) file format.

Physical and radiological properties

CT images were used to evaluate the radiological characteristics of wood samples. Figure 1 shows CT scans of all wood samples in coronal planes.

Hounsfield units (HUs)

The CT number is expressed in terms of HU and estimated from the linear transformation of the estimated attenuation coefficients based on the arbitrary definitions of air and water i.e. at STP the radio-density of distilled

water and air were 0 HU and -1000 HU respectively (Hounsfield, 1980; Rosenblum et al., 1980).

The CT number can be communicated in terms of HU for a voxel of the average linear attenuation coefficient of μ

$$HU_{material} = \frac{(\mu_{material} - \mu_{water})}{\mu_{water}} \times 1000 \quad (1)$$

where HU represents the CT number of a given material and $\mu_{material}/(\mu_{water})$ is the proportion of a particular material's linear attenuation to water (Rosenblum et al., 1980).

Mass density (MD)

The physical mass density of all wood samples was also measured by the weight of known sample volume. Mathematically, mass density is expressed using the following formula (Kishore et al., 2020).

$$\rho = \frac{M}{V} \quad (2)$$

Where: ρ = mass density, M = mass of the fluid or solid V= volume of the fluid or solid Mass density is also calculated from the relation between HU and mass density relationship

$$HU = 1000 \left[\left(\frac{\rho}{\rho_{water}} \right) - 1 \right] \quad (3)$$

Where ρ was the density of material and ρ_{water} was the density of water (Kishore et al., 2020).

Relative electron density (RED)

HU numbers were used to estimate the electron density of the material relative to water using the following relationship [10].

$$\text{Relative electron density (RED)} = \left(\frac{[HU]_{material}}{1000} \right) + 1 \quad (4)$$

Measurement Procedure

When an X-ray strikes a medium attenuation occurs, attenuation refers to both absorption and scattering. Coherent scattering, photoelectric effect, Compton scattering, and pair production are the four major modes of interaction to understand the attenuation process. Heavy-charged particles (alpha and protons), light-charged particles (electron and positrons), and x-rays and gamma rays all interact differently with matter.

The interaction of X-rays with the medium is determined by the energy of the X-rays and the physical and chemical properties of the medium (Kishore et al., 2020). X-rays come under electromagnetic radiation, get attenuated while traversing matter, and follow an exponential law:

$$I = I_0 e^{-\mu x} \quad (5)$$

Where μ is the attenuation coefficient of attenuating material, I is the intensity, I_0 is the initial intensity of the radiation beam, and x is the depth of the attenuating material (Attix, 2008; Kishore et al., 2020).

A/C was employed to keep the sample's irradiation environment at or near standard pressure and temperature requirements. Before starting the measurements, the test run was performed (warm it up). The X-rays were obtained from LINAC and measurements were performed with the help of a Semi-flux ion-chamber (IC) (PTW dosimetry, Germany T10008) volume of 0.125cc and UNIODOS E universal dose-electrometer (PTW dosimetry, Germany T10008). An IC of 0.125cc volume is good enough and recommended to be used for measuring the radiation energy deposited in a medium with high precision. As shown in the Figure.2 a Semi-flux IC was placed on the couch along with a build-up cap made of brass, and connected to the UNIODOS E electrometer with a high-impedance tri-axial cable. A brass Build-up cap was used to establish the charged-particle equilibrium in the air as per the Brag-Grey cavity theorem (Andreo et al., 2002).

Semi-flex IC along with tri-axial cable and electrometer was calibrated from secondary standards dosimetry laboratory (Bhabha Atomic Research Centre, Mumbai, India). A state-of-art Versa HD- linear accelerator (Linac) (Elekta Medical System, UK) was used to generate the x-rays of 6, 10, and 15 mega-volts (MV), in addition to an unfiltered beam of 6 MV (6FFF; flattening filter free) was also used for the study purpose. Linac was calibrated as per the international guidelines prescribed by Technical Reports Series No. 398 of the International Atomic Energy Agency (IAEA). The attenuation properties of wood samples for the above-mentioned photon energies were carried out for collimator opening of 3 x 3 cm², 5 x 5 cm², 10 x 10 cm², and 15 x 15 cm² at a source-to-surface distance (SSD) of 110 cm. Measurements were collected for 100 monitor units (MUs) of each photon beam. Measurements were taken with and without samples kept between the X-ray source and the IC. The attenuation of wood samples was computed using the following formulae (Kumar et al., 2019).

Percentage attenuation calculated as:

$$\% \text{Attenuation} = \left(\frac{\text{Electrometer reading without sample} - \text{electrometer reading with sample}}{\text{Electrometer reading without sample}} \right) \times 100 \quad (6)$$

Results

Physical and Radiological Properties

Table 3 summarizes the radiological properties of wood samples used in the study. The measured radiological properties were; for Acacia Nilotica (HU: -232 ± 40, RED: 0.738 ± 0.039, MD: 0.768 ± 0.024, PD: 0.761), Mangifera Indica (HU: -368 ± 41, RED: 0.662 ± 0.047, MD: 0.632 ± 0.024, PD: 0.632), Azadirachta Indica (HU: -334 ± 44, RED: 0.639 ± 0.042, MD: 0.666 ± 0.025, PD: 0.703), Tectona Grandis l (HU: -370 ± 61, RED: 0.604 ± 0.059, MD: 0.630 ± 0.036, PD: 0.694), Ficus Religiosa (HU: -443 ± 39, RED: 0.543 ± 0.038, MD: 0.608 ± 0.035, PD: 0.576), Tecomella Undulata (HU: -382 ± 54, RED: 0.500 ± 0.052, MD: 0.618 ± 0.035, PD: 0.761), Sesamum Indicum (HU: -292 ± 68, RED: 0.680 ± 0.066, MD: 0.747 ± 0.035, PD: 0.747), and Pinus (HU: -298 ± 27, RED: 0.680 ± 0.229, MD: 0.702 ± 0.131, PD: 0.588), respectively.

Physical dimensions and their masses are measured in all wood samples which are mentioned in Table 2.

Table 1. Effects of Radiation on Various Regions of the Human Body

S No.	Organ	Effect
1	Hair	Baldness and hair follicle loss
2	Brain	Fatigue, nausea
3	Bone marrow and WBC	Immune system failure
4	Intestine Lining	Diarrhea and malnutrition
5	Body	DNA cleavage
6	Uterus	Destruction of eggs

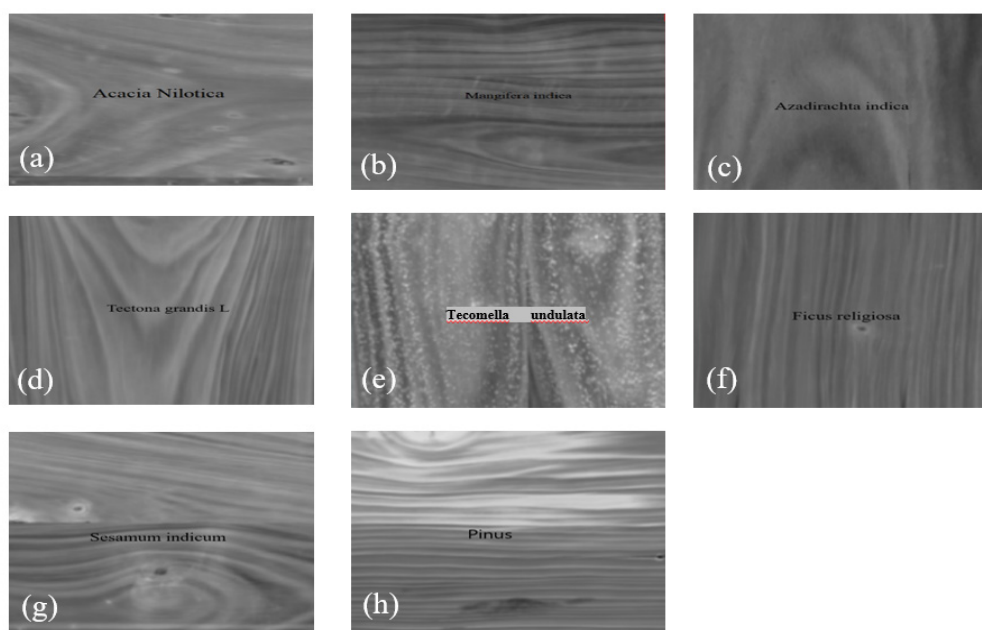


Figure 1. Computed Tomographic Images of (a) acacia nilotica, (b) Mangifera indica, (c) azadirachta indica, (d) tectona grandis l, (e) Tecomella undulata, (f) ficus religiosa, (g) sesamum indicum and (h) pinus respectively.

Table 2. Estimated Radiological Properties of Wooden Samples Using the CT-Images (mean \pm SD).

S N	Wood samples	Hounsfield Units (HU)	Relative electron density (RED)	Mass density (g/cc ³)	Physically measured Mass Density (g/cc)
1	Acacia Nilotica	-232 \pm 40	0.738 \pm 0.039	0.768 \pm 0.024	0.761
2	Mangifera indica	-368 \pm 41	0.662 \pm 0.047	0.632 \pm 0.024	0.632
3	Azadirachta indica	-334 \pm 44	0.639 \pm 0.042	0.666 \pm 0.025	0.703
4	Tectona grandis L	-370 \pm 61	0.604 \pm 0.059	0.630 \pm 0.036	0.694
5	Ficus religiosa	-433 \pm 39	0.543 \pm 0.038	0.608 \pm 0.035	0.576
6	Tecomella undulata	-382 \pm 54	0.500 \pm 0.052	0.618 \pm 0.035	0.671
7	Sesamum indicum	-292 \pm 68	0.680 \pm 0.066	0.747 \pm 0.035	0.747
8	Pinus	-298 \pm 227	0.680 \pm 0.229	0.702 \pm 0.131	0.588

SD, Standard deviation



Figure 2. Experimental Setup of Ion-Chamber (IC) under LINAC Head.

The measured physical mass density of Acacia Nilotica, Mangifera Indica, Azadirachta Indica, Tectona Grandis L, Ficus Religiosa, Tecomella Undulata, Sesamum Indicum, and Pinus were 0.761 g/cc, 0.632 g/cc, 0.703 g/cc, 0.694 g/cc, 0.576 g/cc, 0.671 g/cc, 0.747 g/cc and 0.588 g/cc respectively. The measured physical mass densities of wood samples were in congruence with the computed mass density of the respective wood sample using CT data.

Attenuation analysis

The Acacia Nilotica has a high density (0.761g/cc) and Ficus religious has a low density (0.576g/cc) among the wood sample used in the study. Hence, Acacia Nilotica wood was found to have maximum attenuation and Ficus Religiosa has minimum attenuation for X-rays of 6 MV, 10 MV, 15 MV, and 6 FFF beams. Figure 3 illustrates the

measured attenuation of wood samples plotted against different collimator openings for 6 MV, 10 MV, 15 MV, and 6 FFF photon energies, respectively.

Discussion

The present study experimentally investigates the radiological properties (i.e. HUs, RED, and MD) of Acacia Nilotica, Mangifera Indica, Azadirachta Indica, Tectona Grandis L, Ficus Religiosa, Tecomella Undulata, Sesamum Indicum, and Pinus wood. It is observed that Acacia Nilotica wood has a high mass density compared to the other wood samples under study. Hence, Acacia Nilotica has higher absorption for X-ray beams of 6 MV, 10 MV, 15 MV, and 6 FFF energies, for all beam openings respectively. It was also observed that there was a slight decrease in attenuation with an increase in field opening. This can be attributed using the fact that, there is an increase in the scatter component of the X-ray beam with an increase in beam opening. It was also observed that there was a decrease in attenuation of the X-ray beam with an increase in X-ray beam energy. This can be attributed using the fact that, a high-energy X-ray beam has a more forward peak spectrum compared to low energy X-ray beam. Therefore, a high-energy X-ray beam has more penetration power compared to the low energy X-ray beam. 6 FFF X-ray beam has softer components compared to 6 MV, 10 MV, and 15 MV beams. Thus, the 6 FFF beam has more attenuation compared to counterpart X-ray beams, for all wood samples used in the study. Rajasekhar et al., (2014) reported that Acacia Nilotica wood has a high mass attenuation coefficient (causes higher attenuation)

Table 3. Wood Samples Used under Study along with Their Physical Properties

SN	Scientific Name	Common Name	Family	Type	Length (cm)	Width (cm)	Thickness (cm)	Volume (cc)	Mass (gm)	Density (g/cc)
1	Acacia Nilotica	Babul	Mimosoideae	Hardwood	20	20	1.7	680	518	0.761
2	Mangifera indica	Mango	Anacardiaceae	Hardwood	20	20	1.7	680	430	0.632
3	Azadirachta indica	Neem	Meli.aceae	Hardwood	20	20	1.7	680	478	0.758
4	Tectona grandis L	Saagon	Lamiaceae	Hardwood	20	20	1.7	680	472	0.694
5	Ficus religiosa	Pippal	Mulberry	Hardwood	20	20	1.7	680	392	0.576
6	Tecomella undulata	Rohinda	Bignoniaceae	Hardwood	20	20	1.7	680	456	0.67
7	Sesamum indicum	Seesam	Pedaliaceae	Hardwood	20	20	1.7	680	508	0.747
8	Pinus	Cheed /Pine	Pinaceae	Hardwood	20	20	1.7	680	400	0.588

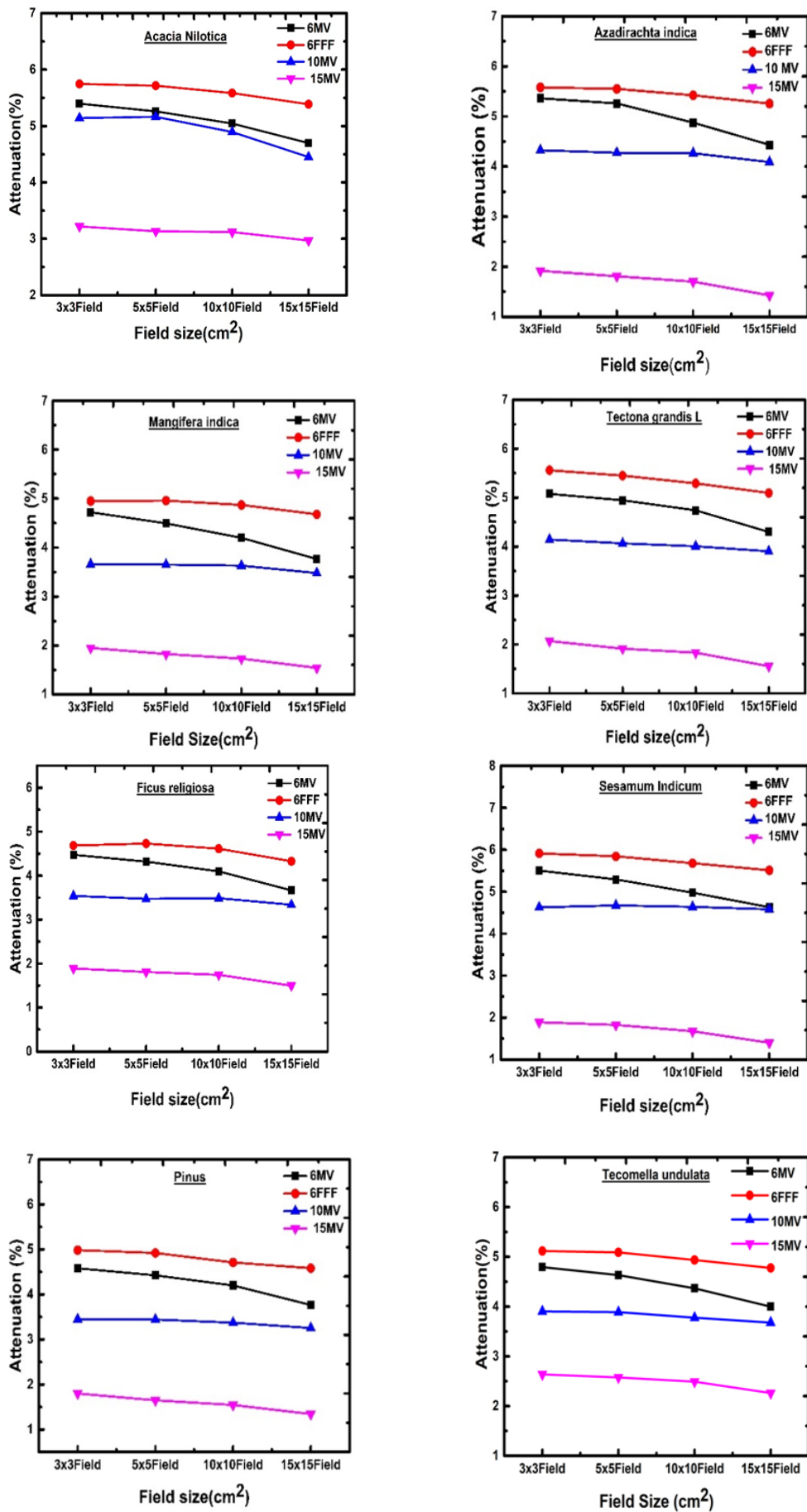


Figure 3. Attenuation of X-rays of 6 MV, 6 FFF, 10 MV and 15 MV Energies for (a) acacia nilotica, (b) azadirachta indica, (c) mangifera indica, (d) tectona grandis l, (e) ficus religiosa, (f) sesamum indicum, (g) pinus and (h) Tecomella undulata wood samples, respectively

using a gamma spectrometer NaI scintillator detector in the energy range of 0.511 MeV to 1.332 MeV. Aung et al., (2019) investigated the radiological properties of various wood (Tectona Grandis Linn (teak), Hevea braziliensis (rubber), Xylia Delabritormis (ironwood), Dipterocarpus Baudii (Keruing), Gmelina Arborea (Yamane), Pinus (Pine) and Albizia Lebbeck (rain tree) and reported that Keruing wood has the highest density and rain tree has minimum.

Barman et al., (2022) investigated 11 wood species of varying density namely., Samanea Saman, Albizia Procera, Gmelina Arborea, Swietenia Mahagoni, Mangifera Indica, Acacia, Auriculiformis, Artocarpus Heterophyllus, Aegle Marmelos, Vachellia Nilotica, Tectona Grandis and Syzygium Cumini, they reported that the Aegle Marmelos wood is the most effective, whereas Mangifera Indica is the least effective for fast neutron attenuation amongst 11 wood species Barman et al., (2022) concluded that wood rich in hydrocarbons and low Z materials is a more suitable candidate for fast neutron attenuation, as hydrogen element plays a vibrant role in fast neutron attenuation.

Radiation attenuation is dependent on the incident radiation energy and the composition of the wood, according to Ero et al., (2011) who used the gamma scintillation detection method to study 22 wood samples and found Ayin (highest attenuation) and Araba (lowest attenuation). Heavy materials like lead (Pb) and Pb-containing materials (PbO and Pb₂O₃) are the most commonly used shielding material. Owing to the hazardous nature of Pb, it could affect the human, animal, plant, and eco-system as well (Liu et al., 2014; Warniment et al., 2010; Reis et al., 2010). Therefore, there is an ongoing surge to find alternative materials.

Poltabtım et al., (2021) reported that wood polyvinyl chloride (WPVC) composite with Bismuth oxide (Bi₂O₃) is a good alternative to Pb. Other developed Pb-free composites are namely viz; W/Bi₂O₃/methyl vinyl silicon rubber (Singh et al., 2017), W₂O₃/ethylene propylene diene monomer (Chai et al., 2016) Bi₂O₃/W/natural rubber (Poltabtım et al., 2018), Bi/high-density polyethylene (Poltabtım et al., 2021), etc. with varying attenuation properties depending upon their composition, type, and manufacturer. Apart from this, Gurjar et al., (2015) and Kumar et al., (2011) reported the use of wood of different densities (Racemosa: 0.212 g/cc, Pinewood: 0.329 g/cc, and Kail wood: 0.420 g/cc) as a phantom material to introduce inhomogeneity in the medium for the quantification of alternation in the radiation energy deposited in the medium. The movable X-ray shielding panels, radiation housing doors, and transportation casks entail lightweight material, wood in combination with other materials can provide a solution. Graphene/WPC Zhang et al., (2015) and Ni/W/PVC Chen, et al., (2018) have been used for electromagnetic (EM) interference shield material for EM waves of frequency of the order of 60 MHz-1.5GHz and 8.2 GHz-12.4 GHz, respectively. Bucur (2003) highlighted the need for wooden technology, to develop a non-destructive and non-contact technique to sustain the structural integrity of the wooden sample for in-vivo and in-situ measurements.

Hence, wood has multiple roles in radiation shielding,

inhomogeneous phantom fabrication for radiation dose measurement in radiation therapy, and designing the EM shield material. Therefore, a continuous effort should be made to explore the radiological properties of locally available wood. This can be a cost-effective and easy solution to all the above-mentioned needs. In the present study, it can be concluded that Acacia Nilotica has higher absorption for X-ray beams of 6 MV, 10 MV, 15 MV, and 6 FFF energies, for all beam openings respectively.

In conclusion, according to the findings of this study, radiation attenuation in wood samples is affected by incident photon energy, wood type, and Collimator opening. Its rise in relation to density diminishes as energy increases. Acacia Nilotica has the highest radiation attenuation, whereas Ficus Religiosa has the lowest. Various radiological parameters were determined for wood samples that can be utilized to create inhomogeneous phantoms for dosimetry. Because environmental protection is becoming increasingly important in our daily lives, it is recommended that further research on the shielding qualities of materials be done, as well as the utilization of more unknown tropical woods. Wood is fairly inexpensive and readily available in the nearby area.

Author Contribution Statement

Sonal Varshney and Lalit Kumar contributed to investigation, writing, analysis and drafted the manuscript. Umesh Kumar Diwedi contributed for conceptualization, analysis, methodology and figures preparation. Pradeep Narayan worked as a supervisor in-charge. The manuscript was reviewed by all of the authors.

Acknowledgements

The authors would like to express their gratitude to the management of the Department of Radiation Oncology at the All India Institute of Medical Sciences in Jodhpur, India, for their ongoing support and encouragement in completing this research.

Availability of data

The corresponding author will provide the datasets used and/or analyzed during the study upon reasonable request.

Ethical Approval

Not applicable because the study did not contain any human or animal studies.

Conflict of Interest

None.

References

- Attix FH (2008). Introduction to radiological physics and radiation dosimetry. John Wiley & Sons, WILEY-VCH Verlag GmbH & Co.KGaA, pp 1-10.
- Aung YY, Tun KT (2019). Investigation of Gamma Radiation Shielding Characteristics for Various Wood Slabs by Using Gamma Attenuation Method. *Int J Adv Eng Res Sci*, **43**,

- 99-102.
- Andreo P, Huq MS, Westermark M, et al (2002). Protocols for the dosimetry of high-energy photon and electron beams: a comparison of the IAEA TRS-398 and previous international Codes of Practice. *Phys Med Biol*, **47**, 3033.
- Barman R, Hossain MS, Das A, Rabby MKA (2022). Investigation of radiation shielding characteristic features of different wood species. *Radiat Phys Chem*, **192**, 109927.
- Bucur V (2003). Nondestructive characterization and imaging of wood. Springer Science & Business Media.
- Bucur V (2003). Ultrasonic imaging of wood structure. In Proceedings of 5th world conference in ultrasonics, Paris, 299-302.
- BOARD SS (1996). Task Group On The Biological Effects Of Space Radiation.
- Chen J, Teng Z, Zhao Y, Liu W (2018). Electromagnetic interference shielding properties of wood-plastic composites filled with graphene decorated carbon fiber. *Polym Compos*, **39**, 2110-6.
- Chai H, Tang X, Ni M, et al (2016). Preparation and properties of novel, flexible, lead-free X-ray-shielding materials containing tungsten and bismuth (III) oxide. *J Appl Polym Sci*, **133**.
- Charles MW (2008). ICRP Publication 103: Recommendations of the ICRP.
- Ero FA, Adebo BA (2011). Determination of gamma radiation shielding characteristics of some woods in western Nigeria. *Int Arch Sci Technol*, **3**, 14-20.
- Gurjar OP, Mishra PK, Singh N, Bagdare P, Mishra SP (2015). Dosimetric study for the development of heterogeneous chest phantom for the purpose of patient-specific quality assurance. *Radiat Protect Environ*, **38**, 139.
- Hounsfield GN (1980). Computed medical imaging. Nobel lecture, December 8, 1979. *J Comput Assist Tomogr*, **4**, 665-74.
- Martin A, Harbison S, Beach K, Cole P (2018). An introduction to radiation protection. Crc Press.
- Rajasekhar E, Kumar RJ (2014). Experimental investigation of gamma radiation shielding characteristics of wood. *Int J Humanit Soc Sci*, **2**, 21-26.
- International Atomic Energy Agency (2006). Radiation protection in the design of radiotherapy facilities. Internat. Atomic Energy Agency.
- Kumar L, Kishore V, Bhushan M, Kumar P, Kumar G (2022). Design and fabrication of a thoracic phantom for radiation dose verification in mega-voltage X-ray beam. *Mater Today Proc*, **49**, 3050-5.
- Kishore V, Kumar L, Bhushan M, Yadav G (2020). A study for the development of a low density heterogeneous phantom for dose verification in high energy photon beam. *Radiat Phys Chem*, **170**, 108638.
- Kumar L, Yadav G, Kishore V, Bhushan M (2019). Dosimetric validation of Acuros XB photon dose calculation algorithm on an indigenously fabricated low-density heterogeneous phantom. *Radiat Protect Environ*, **42**, 173.
- Kumar A, Sharma SD, Arya AK, Gupta S, Shrotriya D (2011). Effect of low-density heterogeneities in telecobalt therapy and validation of dose calculation algorithm of a treatment planning system. *J Med Phys*, **36**, 198.
- Liu G, Yu Y, Hou J, et al (2014). An ecological risk assessment of heavy metal pollution of the agricultural ecosystem near a lead-acid battery factory. *Ecol Indic*, **47**, 210-8.
- Poltabtim W, Wimolmala E, Markpin T, et al (2021). X-ray shielding, mechanical, physical, and water absorption properties of wood/PVC composites containing bismuth oxide. *Polymers*, **13**, 2212.
- Poltabtim W, Toyen D, Saenboonruang K (2021). Theoretical determination of high-energy photon attenuation and recommended protective filler contents for flexible and enhanced dimensionally stable wood/NR and NR composites. *Polymers*, **13**, 869.
- Poltabtim W, Wimolmala E, Saenboonruang K (2018). Properties of lead-free gamma-ray shielding materials from metal oxide/EPDM rubber composites. *Radiat Phys Chem*, **153**, 1-9.
- Reis LSLDS, Pardo PE, Camargos AS, Oba E (2010). Mineral element and heavy metal poisoning in animals. *J med med Sci*, 560-79.
- Rosenblum LJ, Mauceri RA, Wellenstein DE, et al (1980). Density patterns in the normal lung as determined by computed tomography. *Radiology*, **137**, 409-16.
- Singh AK, Singh RK, Sharma B, Tyagi AK (2017). Characterization and biocompatibility studies of lead free X-ray shielding polymer composite for healthcare application. *Radiat Phys Chem*, **138**, 9-15.
- Warniment C, Tsang K, Galazka SS (2010). Lead poisoning in children. *Am Fam Physician*, **81**, 751-7.
- Zhang Y, Fang XX, Wen BY (2015). Asymmetric Ni/PVC films for high-performance electromagnetic interference shielding. *Chinese J Polym Sci*, **33**, 899-907.



This work is licensed under a Creative Commons Attribution-Non Commercial 4.0 International License.